INSTITUTE OF PHYSICS PUBLISHING JOURNAL OF PHYSICS D: APPLIED PHYSICS

J. Phys. D: Appl. Phys. **34** (2001) 1745–1755 www.iop.org/Journals/jd PII: S0022-3727(01)20179-X

# Role played by the $N_2(A\,^3\Sigma_u^+)$ metastable in stationary $N_2$ and $N_2$–$O_2$ discharges

**V Guerra**[1], **P A Sá**[2] **and J Loureiro**[1]

[1] Centro de Física dos Plasmas, Instituto Superior Técnico, 1049-001 Lisboa, Portugal
[2] DEEC, Faculdade de Engenharia, Universidade do Porto, 4200-465 Porto, Portugal

Received 18 December 2000

**Abstract**

The role played by the $N_2(A\,^3\Sigma_u^+)$ metastable on the overall kinetics of $N_2$ and $N_2$–$O_2$ stationary discharges is illustrated by using a kinetic model based on the self-consistent solutions to the Boltzmann equation coupled to the rate balance equations for the vibrationally and electronically excited molecules, atoms and charged particles, in which the sustaining electric field is self-consistently determined. It is shown that together with the vibrational distribution of $N_2(X\,^1\Sigma_g^+, v)$ molecules, the metastable state $N_2(A\,^3\Sigma_u^+)$ plays a central role in the whole problem, since some important aspects of these discharges, such as ionization, gas phase chemistry and gas heating are associated with different processes involving the $N_2(A\,^3\Sigma_u^+)$ state.

## 1. Introduction

In a gas discharge the metastable states may be strongly populated. Moreover, due to their extended lifetime they are able to store energy for a long time, and they will eventually release this energy through different channels. It is easy to imagine some possible paths for the energy available from the metastable states. The first one is ionization: on the one hand it requires less energy to ionize a molecule by electron impact from a metastable state than from the ground level, so that stepwise ionization may take place in the case of appreciable populations of the metastables; on the other hand the metastable species may store enough energy to directly ionize the gas, by Penning or associative ionization. The second one is plasma chemistry: the metastable states may transfer their energy to other species present in the discharge, giving rise to different chemical reactions and hence possibly enabling certain species may be created. Finally, if the metastable states release their energy to the background gas they play a role in the gas heating.

In the case of nitrogen, the first electronically excited metastable state is the triplet $A\,^3\Sigma_u^+$, with an energy threshold of 6.2 eV and with a lifetime close to 2 s. Owing to the above stated reasons, the $N_2(A)$ state may play a central role in the elementary processes that control a nitrogen discharge. However, in nitrogen the main energy reservoirs are not the electronic metastables, but instead the vibrational levels of the $N_2(X\,^1\Sigma_g^+)$ state, so that a first attempt to understand the kinetics of a nitrogen discharge consists in studying the coupling between the electrons and the vibrational states. This is often a good approach, but the aim of this paper is to call attention to the fact that the metastable states are also present, and that they may and they do play a role as well.

Electrical discharges in nitrogen and in mixtures containing nitrogen are of interest to various fields, such as atmospheric chemistry, the re-entry of space vehicles [1] and the surface treatment of materials [2]. In the last few years many articles have been published devoted both to the experimental characterization of discharges in $N_2$ and in $N_2$–$O_2$ (e.g., [3, 4]) and to the development of kinetic models for these discharges. Theoretical works have been developed emphasizing different aspects of the discharge and using different degrees of sophistication. For example, pioneering investigations on the strong coupling between the electron energy distribution function (EEDF) and the vibrational distribution function (VDF) of $N_2(X\,^1\Sigma_g^+, v)$ molecules in nitrogen can be found in [5, 6], whereas the coupling of the EEDF and the VDF with the electronic states has been analysed in [7, 8], the effects of vibrational deactivation of the VDF on the wall was studied in [9] and a full self-consistent model for the whole kinetics in $N_2$ was presented in [10]. Furthermore, kinetic models for discharges in $N_2$–$O_2$ have been presented in [11–16], starting from essentially experimental works with only a simplified kinetic scheme, in which the electron kinetics was taken into account in a simple way [11], to the rather complete model presented in [16]. On the other hand, the kinetics of the metastable state $N_2(A\,^3\Sigma_u^+)$ in discharges containing nitrogen has also been the subject of many works. As examples, the elementary kinetics of $N_2(A)$ has been studied in [17–21], the importance of this state in the excitation of $N_2(C)$ in a post discharge has been investigated in [22], the need for the study of $N_2(A\,^3\Sigma_u^+)$ in order to interpret

  

the nitrogen afterglow has been stressed in [23], while absolute measurements of the metastable molecules using intracavity laser absorption spectroscopy were recently obtained in [24]. Therefore, many articles have been published related either to the study of discharges in $N_2$ and $N_2$–$O_2$ or to the kinetics of $N_2(A\,^3\Sigma_u^+)$ metastables. However, an ensemble view is still missing. The purpose of this work is to use many of the data reported in the literature and, together with some new results, clearly point out in a unified way the role of the $N_2(A\,^3\Sigma_u^+)$ state in the overall physics of the discharge.

The contribution of the present paper to this field is to report the main results of an extended kinetic study based on the solutions of a stationary self-consistent model that couples the electron Boltzmann equation to the rate balance equations for the most important neutral and ionic species present in the discharge. The reduced maintenance electric field is also determined in the model from the electron balance equation, coupled to those for the main positive ions, using the requirement that under steady-state conditions the total rate of ionization must compensate exactly for the rate of electron loss by ambipolar diffusion to the wall plus electron–ion recombination. The system under analysis is a steady-state plasma column created in a discharge tube of inner radius ∼1 cm, operating at pressures around 1 Torr, either in direct current (dc) or microwave fields.

The description of the model has been presented in [10] for the case of a discharge in pure nitrogen and in [15, 16] for a discharge in an $N_2$–$O_2$ mixture, so the reader should refer to these papers for details. Nevertheless, we briefly review in section 2 the main aspects involved in the kinetics of these discharges. The theoretical predictions and the corresponding discussion are presented in section 3. Finally, section 4 summarizes the main conclusions.

## 2. Theoretical formulation

The model developed ensures a self-consistent description of the kinetic processes occurring in a low-pressure dc or microwave discharge, providing an important insight into the basic properties of such a system. The input parameters of the model are the common discharge operating parameters, namely gas pressure, discharge current (dc case) or electron density (microwave discharge), field frequency and tube radius. Except for the final part of this paper, where the gas thermal balance equation is also incorporated in the system of equations, the gas temperature is used as an input parameter.

### *2.1. Electron kinetics*

The EEDF is calculated by solving the homogeneous Boltzmann equation using the two-term expansion in spherical harmonics. For the case of a microwave discharge we assume the effective field approximation [25], under which the angular field frequency $\omega$ is assumed sufficiently high so that the EEDF is nearly stationary. The effects produced by e–e Coulomb collisions are taken into account following the same procedure as in [26].

Basically, the electron cross sections used in this work are the same as reported in previous papers for discharges in $N_2$ [10] and in $N_2$–$O_2$ [16]. The electron Boltzmann equation is solved taking into account elastic collisions, excitation and the de-excitation of rotational levels, inelastic and superelastic collisions with vibrationally excited molecules, excitation of the electronic states (of $N_2$, N, $O_2$ and O) and ionization. The excitation of electronic states was treated as a single energy loss process, assuming that all the molecules are in the ground vibrational level. Finally, although the EEDF has not been calculated including the processes of electron–ion recombination and electron attachment (the later in the case of $O^-$ production), since the numerical code employed requires electron number conservation, the rate coefficients for these processes have been determined using the EEDF calculated in the absence of such processes. This procedure introduces only very small errors in the calculation of the EEDF [27].

In a dc discharge the only electron impact processes involving the metastable state $N_2(A\,^3\Sigma_u^+)$ are direct excitation, $e + N_2(X) \rightarrow e + N_2(A)$, and stepwise ionization, $e + N_2(A) \rightarrow e + e + N_2^+$. For a microwave discharge we have further considered the stepwise excitation processes $e + N_2(A) \rightarrow e + N_2(B, C)$ and the superelastic collisions $e + N_2(A) \rightarrow e + N_2(X)$, since in this latter case the concentrations of $N_2(A)$ are usually larger.

### *2.2. Heavy-particle kinetics*

Due to the inclusion of electron superelastic collisions in the Boltzmann equation, collisions between electrons and atomic species, as well as electron dissociation and ionization from other states than the electronic ground state, this equation is coupled to a system of kinetic master equations for the populations of the various neutral species created in the discharge. For a discharge in pure nitrogen, the species to be considered are the vibrational manifold of ground state molecules, $N_2(X\,^1\Sigma_g^+, v)$, the most populated electronic states, $N_2(A\,^3\Sigma_u^+,\ B\,^3\Pi_g,\ C\,^3\Pi_u,\ a'\,^1\Sigma_u^-,\ a'\,^1\Pi_g,\ w'\,^1\Delta_u,\ a''\,^1\Sigma_g^+)$, and the $N(^4S)$ atoms. For the case of the $N_2$–$O_2$ mixture, we considered also the vibrational levels $O_2(X\,^3\Sigma_g^-, v')$, the electronic states $O_2(a'\,^1\Delta_g,\ b'\,^1\Sigma_g^+)$, the $O(^3P)$ atoms and the molecular species $NO(X\,^2\Pi_r)$ and $O_3$. The various processes taken into account in determining the populations of the different species, as well as the choice of the respective rate coefficients, have been discussed in detail in our previous publications [10, 15, 16]. Here, we just recall in tables 1 and 2 the list of the various reactions involved in the kinetics of $N_2(A\,^3\Sigma_u^+)$ in pure nitrogen and in the case of a $N_2$–$O_2$ mixture, respectively.

### *2.3. Maintenance electric field*

The reduced sustaining field in the plasma is self-consistently calculated by solving the continuity equations for the electrons and the various positive ions, under the assumption of a quasineutral discharge. For the case of nitrogen, the positive ions to consider are $N_2^+$ and $N_4^+$, whereas for a discharge in $N_2$–$O_2$ the species $O_2^+$, $O^+$ and $NO^+$ should also be considered. The procedure used to include the effects of negative ions in the calculation of the field has been presented in [16]. For the $N_2$–$O_2$ mixture, the negative ions $O^-$ are important only for a discharge predominantly constituted by $O_2$ [16, 28], so that they will not be considered here.

**Table 1.** Kinetics of the $N_2(A)$ metastable state in a nitrogen discharge.

| | Process | Rate coefficient |
|---|---|---|
| R1 | $N_2(A) \xrightarrow{diffusion} N_2(X, v = 0)$ | $ND = 5 \times 10^{18}\sqrt{T_g(K)/300}$ cm$^{-1}$ s$^{-1}$ |
| R2 | $N_2(A)+N_2(A) \longrightarrow N_2(B) + N_2(X, v = 8)$ | $k = 7.7 \times 10^{-11}$ cm$^3$ s$^{-1}$ |
| R3 | $N_2(A)+N_2(A) \longrightarrow N_2(C) + N_2(X, v = 2)$ | $k = 1.5 \times 10^{-10}$ cm$^3$ s$^{-1}$ |
| R4 | $N_2(B)+N_2 \longrightarrow N_2(A) + N_2(X, v = 0)$ | $k = 0.95 \times 3 \times 10^{-11}$ cm$^3$ s$^{-1}$ |
| R5 | $N_2(A)+N_2(X, 5 \leqslant v \leqslant 14) \longrightarrow N_2(B) + N_2(X, v = 0)$ | $k = 2 \times 10^{-11}$ cm$^3$ s$^{-1}$ |
| R6 | $N_2(B) \longrightarrow N_2(A) + h\nu$ | $\nu = 2 \times 10^5$ s$^{-1}$ |
| R7 | $N_2(A)+N(^4S) \longrightarrow N_2(X, 6 \leqslant v \leqslant 9) + N(^2P)$ | $k = 4 \times 10^{-11}$ cm$^3$ s$^{-1}$ |

**Table 2.** Additional processes involving $N_2(A)$ for a discharge in the mixture $N_2$–$O_2$.

| | Process | Rate coefficient |
|---|---|---|
| R8 | $N_2(A)+O \longrightarrow NO + N(^2D)$ | $k = 7 \times 10^{-12}$ cm$^3$ s$^{-1}$ |
| R9 | $N_2(A)+NO \longrightarrow N_2(X, v = 0)+NO(A)$ | $k = 6.6 \times 10^{-11}$ cm$^3$ s$^{-1}$ |
| R10 | $N_2(A)+O_2 \longrightarrow N_2(X, v = 0) + O_2$ | $k = 8.75 \times 10^{-13}(T_g(K)/300)^{0.55}$ cm$^3$ s$^{-1}$ |
| R11 | $N_2(A)+O_2 \longrightarrow N_2(X, v = 0) + O + O$ | $k = 1.63 \times 10^{-12}(T_g(K)/300)^{0.55}$ cm$^3$ s$^{-1}$ |
| R12 | $N_2(A)+O \longrightarrow N_2(X, v = 0) + O$ | $k = 2.1 \times 10^{-11}$ cm$^3$ s$^{-1}$ |
| R13 | $N_2(B)+NO \longrightarrow N_2(A)+NO$ | $k = 2.4 \times 10^{-10}$ cm$^3$ s$^{-1}$ |

The reduced electric field is determined using the requirement that under steady-state conditions the total rate of ionization must compensate exactly for the rate of electron loss by diffusion to the wall, under space-charge field effects, plus electron–ion recombination. For $n$ different kinds of positive ions and in the absence of the effects produced by negative ions, the electrons and ions are governed by classical ambipolar diffusion, in which the diffusion coefficient for the charged species $i$, $D_{ai}$, is given by

$$D_{ai} = D_i - \mu_i \frac{\sum_{j=1}^{n+1} n_j D_j}{\sum_{j=1}^{n+1} n_j \mu_j} \qquad i = 1, \ldots, n+1. \tag{1}$$

In this equation the index $n + 1$ corresponds to the electrons, $D_i$ and $\mu_i$ are the free diffusion coefficient and the mobility for species $i$, respectively, the latter is assumed positive for the ions and negative for the electrons, and $n_i$ is the concentration of the ionic species $i$, with $n_{n+1} = -n_e$, $n_e$ denoting the electron density. Due to the nature of the continuity equations for charged particles, once the continuity equation for electrons is satisfied for a given value of the reduced electric field, the continuity equation for the sum of the ionic concentrations is also satisfied. In this way, the quasineutrality condition, $\sum_{i=1}^{n+1} n_i = 0$, constitutes an additional constraint to the problem, ensuring that the ionic concentrations may be decoupled.

The total rate of ionization includes both ionization by direct impact on $N_2(X\,^1\Sigma_g^+)$ molecules and stepwise ionization from $N_2(A\,^3\Sigma_u^+)$ and $N_2(a'\,^1\Sigma_u^-)$, as well as reactions for associative ionization due to collisions between two metastable species, $N_2(A) + N_2(a')$ and $N_2(a') + N_2(a')$. In what concerns the $N_2(A\,^3\Sigma_u^+)$ state, this species plays a direct role in the ionization processes through the reactions $e + N_2(A) \rightarrow e + e + N_2^+$ and $N_2(A) + N_2(a') \rightarrow N_4^+ + e$.

### 2.4. Gas temperature

Since the vibrational distribution function of $N_2(X, v)$ molecules and some reaction rate coefficients are strongly dependent on the gas temperature, $T_g$, we have used in the main part of this modelling experimental values for $T_g$ obtained under the same conditions as for the calculations. Nevertheless, in the final part of this paper $T_g$ has been self-consistently determined from the model, by solving the gas thermal balance equation coupled to the system of equations already described. Neglecting axial transport and assuming a parabolic radial profile for the gas temperature, the stationary gas thermal balance equation takes the well known form

$$\frac{8\lambda(T_g)}{R^2}(T_g - T_w) = Q_{in} \tag{2}$$

where $T_w$ denotes the wall temperature, $Q_{in}$ is the mean input power transferred to the translational mode per volume unit and $\lambda$ is the thermal conductivity, taken from [29].

The calculations of the total gas heating (right-hand side term of the gas thermal balance equation) take into account all collision processes that lead to the transfer of energy to the translation mode. For the case of a discharge in pure nitrogen, the different gas heating channels are as follows.

(i) Vibration–vibration (V–V) energy exchange processes in $N_2$–$N_2$ collisions, i.e. non-resonant reactions of the form

$$N_2(X, v) + N_2(X, w-1) \xrightarrow{P_{v,v-1}^{w-1,w}} N_2(X, v-1) + N_2(X, w) \tag{3}$$

to which correspond a mean input power to the translation mode given by

$$Q_{in}^{V-V} = \sum_{v=1}^{45}[N_2(X, v)] \times \sum_{w=1}^{45}[N_2(X, w-1)]P_{v,v-1}^{w-1,w}\Delta E_{v,v-1}^{w-1,w} \tag{4}$$

where $[M]$ is the volume density of species $M$, $P_{v,v-1}^{w-1,w}$ is the rate coefficient for this process, $\Delta E_{v,v-1}^{w-1,w} = 2\hbar\omega\chi_e(w - v)$ is the energy available from this reaction, and $\omega = 4.443 \times 10^{14}$ s$^{-1}$ and $\chi_e = 6.073 \times 10^{-3}$ are the spectroscopic constants for the anharmonic Morse oscillator describing the energies of the vibrational levels, $E_v = \hbar\omega[(v+1/2) - \chi_e(v+1/2)^2]$ [30].

(ii) Vibration–translation (V–T) energy exchange processes in $N_2$–$N_2$ collisions,

$$N_2(X, v) + N_2 \xrightarrow{P_{v,v-1}} N_2(X, v-1) + N_2 \quad (5)$$

with

$$Q_{in}^{V-T} = [N_2]\sum_{v=1}^{45}([N_2(X, v)]P_{v,v-1} - [N_2(X, v-1)]P_{v-1,v})\Delta E_{v,v-1} \quad (6)$$

where $\Delta E_{v,v-1} = \hbar\omega(1 - 2\chi_e v)$.

(iii) Vibration–translation (V–T) energy exchange processes in multi-quantum $N_2$–N collisions,

$$N_2(X, v) + N \xrightarrow{P_{v,w}^{N_2-N}} N_2(X, w < v) + N \quad (7)$$

with

$$Q_{in}^{N_2-N} = [N]\sum_{v=1}^{45}[N_2(X, v)]\sum_{w=0}^{v-1} P_{v,w}^{N_2-N}\Delta E_{v,w} \quad (8)$$

where $\Delta E_{v,w} = \hbar\omega(v - w)[1 - \chi_e(v + w + 1)]$.

(iv) Electron elastic and rotational losses, which are obtained in a standard way from appropriate integrals on the calculated EEDF.

(v) Exothermic pooling reactions of $N_2(A\,^3\Sigma_u^+)$ (reactions R2 and R3 in table 1),

$$N_2(A) + N_2(A) \xrightarrow{k_{R_2}} N_2(B) + N_2(X, v_1) + \Delta E_1 \quad (9)$$

$$N_2(A) + N_2(A) \xrightarrow{k_{R_3}} N_2(C) + N_2(X, v_2) + \Delta E_2 \quad (10)$$

with

$$Q_{in}^{N_2(A)} = [N_2(A)]^2(k_{R_2}\Delta E_1 + k_{R_3}\Delta E_2). \quad (11)$$

The set of the rate coefficients for the V–V and V–T processes has been presented and discussed in [13], whereas reactions (9) and (10) will be discussed in section 3.3.

## 3. Results and discussion

The present kinetic model has been tested and validated by comparing some significant data derived from the calculations with measured data reported in [4, 12, 14, 31–33]. These comparisons were essentially presented in our previous works [10, 15]. Here, we will focus our attention in the role played by the $N_2(A\,^3\Sigma_u^+)$ metastable state in different aspects of the discharge, such as ionization, chemistry and gas heating.

### *3.1. Ionization*

Under non-equilibrium conditions, the reactions of associative ionization of $N_2$ are known to be important in determining the maintenance electric field [34–40]. Recently two dominant tendencies have appeared in the literature concerning associative ionization. One prefers to explain the experimental data by processes involving the VDF of $N_2(X, v)$ molecules [34–36], through the processes

$$N_2(X, v \geqslant 32) + N_2(X, v \geqslant 32) \longrightarrow N_4^+ + e \quad (12)$$

$$N_2(a''\,^1\Sigma_g^+) + N_2(X, v \geqslant 13) \longrightarrow N_4^+ + e \quad (13)$$

while the other emphasizes the ionization channels due to collisions between metastable electronic states [37–39]

$$N_2(A\,^3\Sigma_u^+) + N_2(a'\,^1\Sigma_u^-) \longrightarrow N_4^+ + e \quad (14)$$

$$N_2(a'\,^1\Sigma_u^-) + N_2(a'\,^1\Sigma_u^-) \longrightarrow N_4^+ + e. \quad (15)$$

Reactions (12) and (13) were first proposed in [34, 35] for the interpretation of experimental data in a nitrogen glow discharge. Later on reaction (12) was retracted in [36], by the same authors who proposed it, due to difficulties in providing a satisfactory explanation of new data. Moreover, the VDFs used in those papers are unrealistically overpopulated on levels $v \geqslant 13$, since the actual VDFs obtained from a self-consistent kinetic model exhibit a rapid fall-off at intermediate and higher $v$th levels, mainly as a result of the effects of V–T exchanges in $N_2$–N collisions and due to vibrational deactivation on the wall. Thus, neither (12) nor (13) contribute significantly to ionization under the present discharge conditions. In what concerns reaction (13), our opinion is still reinforced due to the rapid quenching of the $N_2(a''\,^1\Sigma_g^+)$ state, with a rate coefficient equal to $2.3 \times 10^{-10}$ cm$^3$ s$^{-1}$ [41], which suggests that concentrations for this metastable state are always vanishingly small. However, it is worth noting here that reaction (12) may eventually become important in the afterglow, since the high levels of the VDF may become overpopulated in a nitrogen post discharge as a consequence of the effects produced by near-resonant V–V energy exchanges [42].

The rate coefficients of reactions (14) and (15) were first determined in [38], who reported the values $5 \times 10^{-11}$ and $2 \times 10^{-10}$ cm$^3$ s$^{-1}$, respectively. In order to reconcile the results of a kinetic model to the experimental data, the coefficients have been reduced in [39] to $6 \times 10^{-12}$ and $5 \times 10^{-12}$ cm$^3$ s$^{-1}$, respectively. We have found that a better agreement with the electric field measurements reported in [31], for the case of a pure nitrogen dc discharge produced in a Pyrex glass tube of radius $R = 1$ cm, is obtained for the somewhat intermediate values of $10^{-11}$ and $5 \times 10^{-11}$ cm$^3$ s$^{-1}$, for reactions (14) and (15) respectively. This choice also leads to a good agreement between the predicted and measured populations of N($^4$S) atoms and $N_2(A\,^3\Sigma_u^+)$ and $N_2(B\,^3\Pi_g)$ states.

Figures 1(a)–(c) show the comparison between calculations and measurements of the reduced electric field $E/N$ reported in [31] against the product $NR$, with $N$ denoting the neutral gas density, for various values of the discharge current $I$ in the range 10–100 mA. The figures were obtained using different values for the rate coefficients of the two reactions leading to associative ionization by collisions between the metastable states, through reactions (14) and (15), as follows: (a) $5 \times 10^{-11}$ and $2 \times 10^{-10}$ cm$^3$ s$^{-1}$, respectively, as reported in [38]; (b) $6 \times 10^{-12}$ and $5 \times 10^{-10}$ cm$^3$ s$^{-1}$, respectively, as reported in [39]; (c) our choice $10^{-11}$ and $5 \times 10^{-10}$ cm$^3$ s$^{-1}$, respectively, as proposed in [10]. These figures clearly show the correctness of our choice for the rate coefficients of reactions (14) and (15).

In order to better evaluate the importance of associative ionization in nitrogen discharges, figure 2 shows the relative contribution of the different ionization channels to the total ionization rate, for the same conditions as in figure 1. The full

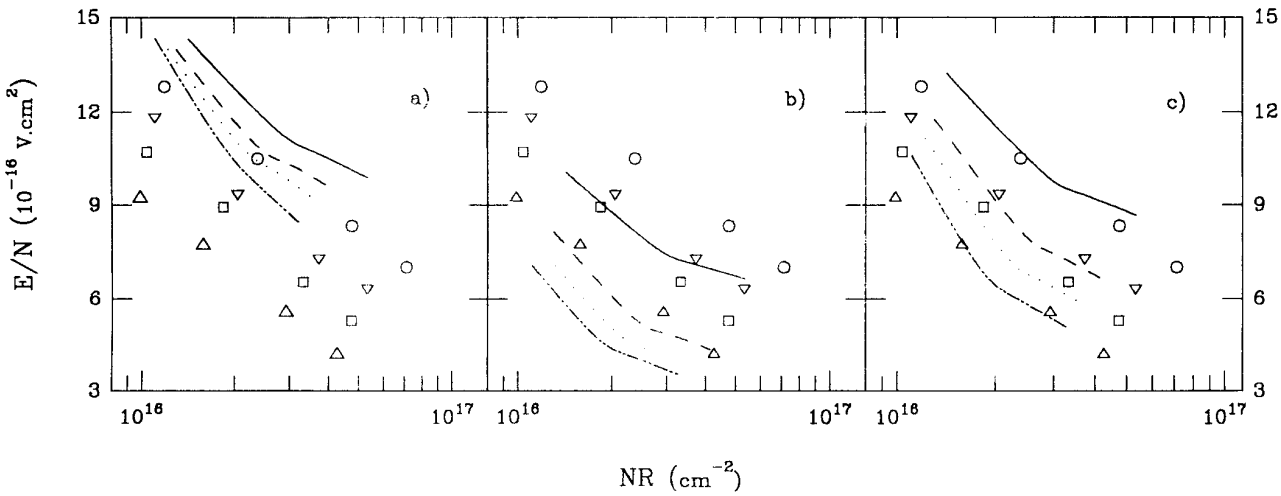


**Figure 1.** Characteristics of $E/N$ against $NR$ for a dc discharge in pure nitrogen with $R = 1$ cm, using the rate coefficients of reactions (14) and (15) reported in (a) [38], in (b) [39], and proposed in our previous work (c) [10]. The upper to lower curves and symbols are for increasing values of $I = 10$, 30, 50 and 100 mA. The symbols correspond to the experimental data from [31].

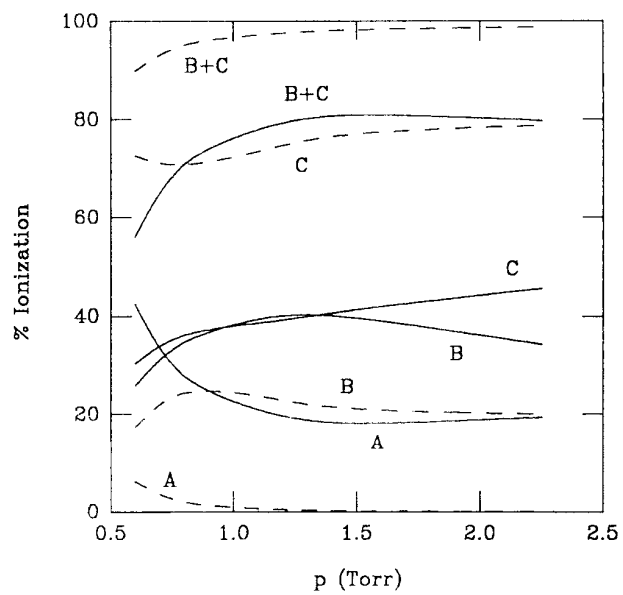


**Figure 2.** Percentage contributions of the various ionization processes against the gas pressure, for a dc discharge in pure nitrogen with $R = 1$ cm and $I = 10$ (full curves) and 100 mA (broken curves), as follows: (A) ionization of $N_2$ by electron impact, $e + N_2 \rightarrow e + e + N_2^+$; (B) associative ionization according to reaction (14), $N_2(A) + N_2(a') \rightarrow e + N_4^+$; (C) associative ionization according to reaction (15), $N_2(a') + N_2(a') \rightarrow e + N_4^+$.

and broken curves correspond to discharge currents of 10 and 100 mA, respectively. When the discharge current rises from 10 to 100 mA, the maintenance reduced electric field decreases (see figure 1), so that the processes of ionization by direct electron impact are less significant, as shown in figure 2. For the conditions here under analysis, associative ionization is the dominant ionization channel, through reactions (14) and (15), and so the metastable states $N_2(A\,^3\Sigma_u^+)$ and $N_2(a'\,^1\Sigma_u^-)$ play a crucial role in establishing the total ionization rate in a nitrogen discharge. On the contrary, the contribution of stepwise ionization to the total ionization rate is always less than 5%.

For the case of a discharge in an $N_2$–$O_2$ mixture, the state $N_2(A\,^3\Sigma_u^+)$ is strongly quenched by $O_2$, O and NO (reactions R8–R12), so that it is no longer able to participate in associative ionization processes (R5, R6). This is shown in figure 3, where we present the relative contribution of the different ionization mechanisms in a dc discharge in $N_2$–$O_2$ at a pressure $p = 2$ Torr, in a tube of radius $R = 0.8$ cm, for discharge currents of $I = 30$ and 80 mA, as a function of the relative oxygen concentration in the mixture. The contribution of associative ionization corresponds to curve E and it rapidly falls from the dominant ionization channel, in a pure nitrogen discharge, to a vanishingly small contribution, even at relative oxygen concentrations as small as ∼15%. As a consequence, the reduced electric field $E/N$ needs to increase when a small amount of oxygen is added into a nitrogen discharge, in order to compensate the reduction of associative ionization, as shown in figure 4. For higher oxygen concentrations, the reduction of $E/N$ with the percentage of oxygen in the mixture is a consequence of the lower energy threshold for direct ionization of $O_2$, as compared to that of $N_2$, together with an enhancement of the high-energy tail of the EEDF, since the total inelastic electron cross section is considerably smaller in $O_2$ than in $N_2$ [13]. We can conclude that, contrary to what happens in a pure $N_2$ discharge, in an $N_2$–$O_2$ mixture the metastable states do not have a significant contribution to the total ionization rate. Nevertheless, close to pure $N_2$, they are responsible for the peculiar behaviour of $E/N$ as a function of the mixture composition shown in figure 4.

### 3.2. Chemistry

We will now discuss the importance of $N_2(A\,^3\Sigma_u^+)$ state in the overall kinetics of the discharge. For the case of pure nitrogen figure 5 shows the calculated and measured relative concentrations $[N_2(A)]/N$ in a dc discharge operating at $p = 0.5, 0.7$ and 1.0 Torr, as a function of the discharge current. The measurements were made by absorption spectroscopy and were taken from [32]. The concordance with the experimental measurements was obtained using mostly collisional and surface data reported in the literature, with the few exceptions

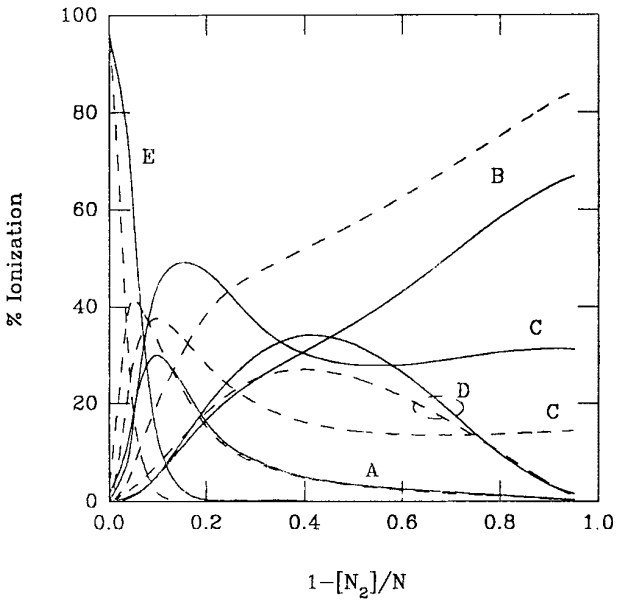


**Figure 3.** Percentage contributions of the various ionization processes against the relative oxygen concentration, in a dc discharge in the mixture $N_2$–$O_2$ for $p = 2$ Torr, $R = 0.8$ cm and $I = 30$ (broken curves) and 80 mA (full curves), as follows: (A) ionization of $N_2$ by electron impact; (B) of $O_2$; (C) of O; (D) of NO; (E) associative ionization in $N_2(A)$+$N_2(a')$ and $N_2(a') + N_2(a')$ collisions.

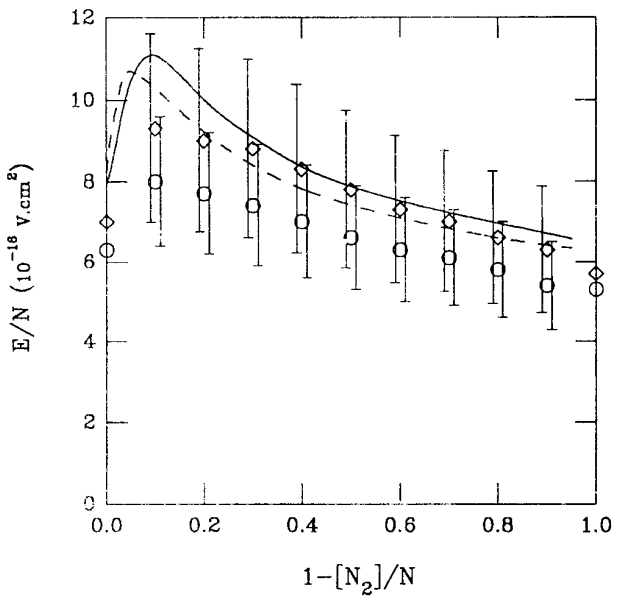


**Figure 4.** Reduced electric field against the relative oxygen concentration, in a dc discharge in the mixture $N_2$–$O_2$ for $p = 2$ Torr, $R = 0.8$ cm and $I = 30$ (– –, ○) and 80 mA (—, ◊). The symbols with error bars correspond to experimental data from [12], for the same conditions as the calculations.

discussed in [10]. It is worth stressing that the populations of $N(^4S)$, $N_2(A)$ and $N_2(B)$ are strongly coupled, through the reactions previously listed in table 1 and rewritten here:

$$N_2(B) + N_2 \longrightarrow 0.95N_2(A) + N_2 \quad (16)$$

$$\longrightarrow 0.05N_2(X) + N_2 \quad (17)$$

$$N_2(A)+N_2(X, 5 \leqslant v \leqslant 14) \longrightarrow N_2(B)+N_2(X, v = 0) \quad (18)$$

$$N_2(A) + N(^4S) \longrightarrow N_2(X, 6 \leqslant v \leqslant 9) + N(^2P). \quad (19)$$

Notice that the rate coefficient for reaction (17) derived in [10], $k = 0.05 \times 3 \times 10^{-11}$ cm$^3$ s$^{-1}$ is close to that reported previously in [43], $k = 2 \times 10^{-12}$ cm$^3$ s$^{-1}$. The strength of the coupling between $N_2(A)$, $N_2(B)$ and $N(^4S)$ can be easily evaluated from figures 6–8.

Figures 6 and 7 show the percentage contributions of the various populating and depopulating mechanisms of $N_2(A\,^3\Sigma_u^+)$ metastables, while figure 8 presents the contributions of the depopulating mechanisms for $N(^4S)$ atoms. Thus, figure 6 shows that the quenching of $N_2(B)$ via reaction (16) is the most important mechanism for creation of $N_2(A)$ metastable. This contribution is by far larger than those due to the radiative decay from $N_2(B)$ and by electron impact on $N_2(X)$. Next, figure 7 shows that the $N_2(A)$ metastables are mainly destroyed through reaction (18), which leads to $N_2(B)$ formation again, and to a smaller extent also by collisions with $N(^4S)$ atoms via reaction (19). The analysis of the various populating and depopulating processes of $N_2(B)$ molecules, not presented here, would reveal again the strong coupling between $N_2(A)$ and $N_2(B)$ states. Therefore, $N_2(A)$ is essentially created and destroyed via $N_2(B)$, so that the combined effects of reactions (16) and (18) do not constitute an effective populating/depopulating mechanism for $N_2(A)$ and $N_2(B)$ states, as they just redistribute an almost constant population among the triplet manifold. In fact, the absolute populations of both these states are actually determined by other slower processes, like reactions (17) and (19), diffusion to the wall and the pooling reactions R2 and R3 (see table 1).

Figure 8 shows the percentage contributions of the various loss processes of $N(^4S)$ atoms as follows: wall reassociation (curves A); effective destruction by electron impact, as a result of the two-step reaction (curves B) $e + N(^4S) \rightarrow e + N(^2D, ^2P)$ followed by collisional and wall destruction of $N(^2D, ^2P)$, which is assumed in the model in a symbolic form as $N(^2D, ^2P) \rightarrow \frac{1}{2}N_2(X, v = 0)$; effective destruction in collisions with the metastable $N_2(A)$ (curves C), also as a result of a two-step reaction $N_2(A) + N(^4S) \rightarrow N_2(X, 6 \leqslant v \leqslant 9) + N(^2P)$ followed by $N(^2P) \rightarrow \frac{1}{2}N_2(X, v = 0)$. The kinetics of the atomic metastable states $N(^2D, ^2P)$ has not been considered in the model, so that it was assumed that most of the atomic metastables give back again a ground-state atom $N(^4S)$ (see [10]). Even if this figure should be just regarded as merely indicative, due to the large uncertainties in the probability for atomic reassociation on the wall and to the simplified treatment of the atomic metastable states $N(^2D, ^2P)$, it shows that the kinetics of $N_2(A\,^3\Sigma_u^+)$ metastables is strongly correlated to that of $N(^4S)$ atoms.

As was shown in the previous section, for the case of a discharge in $N_2$–$O_2$ the metastable state $N_2(A\,^3\Sigma_u^+)$ is strongly destroyed in collisions with O atoms, and $O_2$ and NO molecules, so that it is no longer able to have a significant contribution to the total ionization rate of the discharge. Nevertheless, its concentration remains high enough in order to play a role in some other mechanisms, like reactions R8 and R9 from table 2, rewritten here:

$$N_2(A) + O \longrightarrow NO + N(^2D) \quad (20)$$

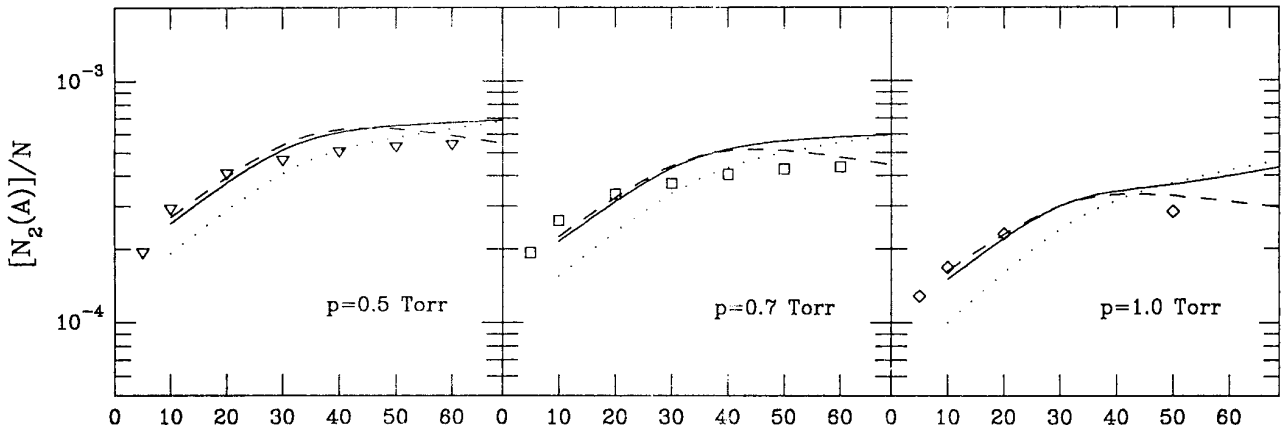


**Figure 5.** Relative concentration of $N_2(A\,^3\Sigma_u^+)$ metastables in a dc discharge in pure nitrogen for $p = 0.5$, 0.7 and 1.0 Torr and $R = 1$ cm, as a function of the discharge current $I$. The different curves correspond to the following choice of the rate coefficients of reactions (14) and (15): (—) present choice; (· · ·) reported in [38]; (– –) reported in [39]. The symbols correspond to experimental data from [32], for the same conditions as the calculations.

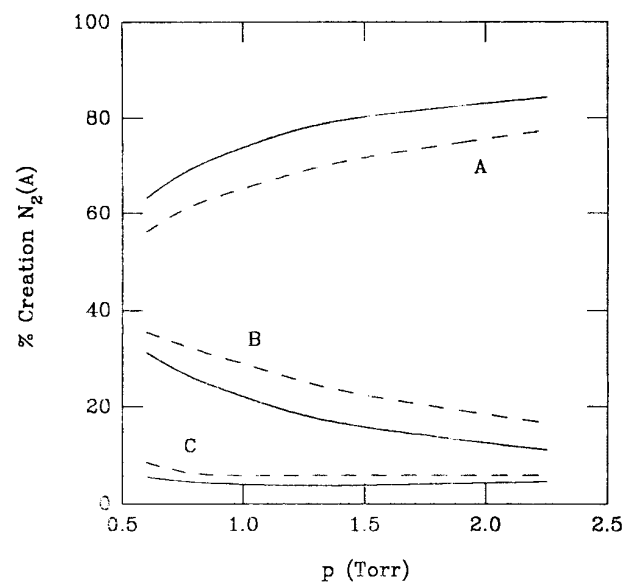


**Figure 6.** Percentage contribution of the various populating mechanisms of $N_2(A\,^3\Sigma_u^+)$ metastables as a function of $p$ and for $I = 10$ mA (full curves) and 100 mA (broken curves), for the same conditions as in figure 5. (A) quenching of $N_2(B)$ via reaction (16); (B) radiative decay from $N_2(B)$; (C) electron impact.

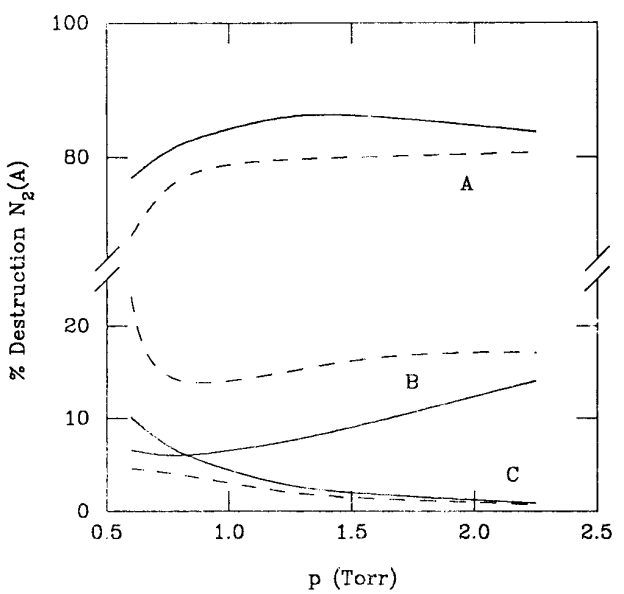


**Figure 7.** Percentage contribution of the various depopulating mechanisms of $N_2(A\,^3\Sigma_u^+)$ metastables as a function of $p$ and for $I = 10$ mA (full curves) and 100 mA (broken curves), for the same conditions as in figure 5. (A) quenching by $N_2(X, v)$ molecules via reaction (18); (B) quenching by $N(^4S)$ atoms (19); (C) diffusion.

$$N_2(A) + NO \longrightarrow N_2(X, v = 0) + NO(A). \qquad (21)$$

Figure 9 shows the percentage contributions of the different mechanisms for the creation of NO, in a dc discharge at $p = 2$ Torr, and $I = 30$ and 80 mA, as a function of the mixture composition, as follows: $N_2(X, v \geqslant 13) + O \rightarrow NO + N$ (curves A); reaction (20), $N_2(A) + O \rightarrow NO + N(^2D)$ (curves B); $N + O_2 \rightarrow NO + O$ (curves C). This figure shows that the populating mechanism of NO involving $N_2(A)$ metastables (curves B) has a non-negligible contribution to the total formation rate of NO, especially at the higher values of the discharge current. Furthermore, the importance of reaction (20) is actually still larger than that shown in figure 9, since the dominant reaction for creation of NO molecules, $N_2(X, v \geqslant 13) + O \rightarrow NO + N$, is almost fully cancelled by the reverse reaction, $NO + N \rightarrow N_2(X, v \simeq 3) + O$. As a consequence of this, the populations of N and NO are strongly coupled to each other, dictating that the absolute value of NO is dependent on other reactions with smaller absolute rates, such as reaction (20), in an effect similar to that occurring in pure nitrogen with $N_2(A)$ and $N_2(B)$ states through reactions (16) and (18).

One of the more intense emissions in an $N_2$–$O_2$ discharge is the NO($\gamma$) 237 nm band, corresponding to the transition NO(A)→NO(X). Figure 10 shows the calculated rate for production of the $NO(A\,^2\Sigma^+)$ state together with the measured relative intensity of the NO($\gamma$) 237 nm band. The predicted and the measured relative concentrations of NO(A) were normalized at $I = 30$ mA and $1 - [N_2]/N = 0.3$. Since the NO(A) state is created here exclusively via reaction (21), the agreement shown in figure 10 is a test of the correctness of the concentrations $[N_2(A)]$ derived using our model.

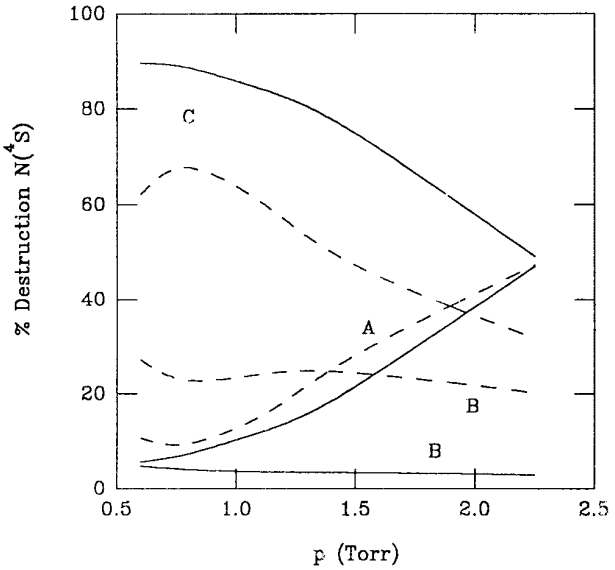


**Figure 8.** Percentage contribution of the various depopulating mechanisms of N($^4$S) atoms as a function of $p$ and for $I = 10$ mA (full curves) and 100 mA (broken curves), for the same conditions as in figure 5. (A) wall reassociation; (B) effective destruction by electron impact (see text); (C) effective destruction by $N_2(A)$ metastables (see text).

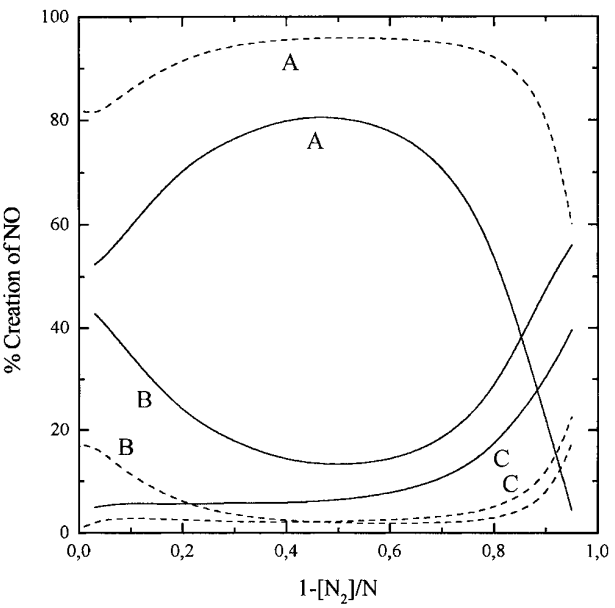


**Figure 9.** Percentage contribution of the various populating mechanisms of NO molecules as a function of the mixture composition, for a $N_2$–$O_2$ dc discharge at $p = 2$ Torr, $R = 0.8$ cm and for $I = 30$ mA (broken curves) and 80 mA (full curves): (A) $N_2(X, v \geqslant 13) + O \rightarrow NO + N$; (B) $N_2(A) + O \rightarrow NO + N(^2D)$; (C) $N + O_2 \rightarrow NO + O$.

Another chemical process in which $N_2(A\,^3\Sigma_u^+)$ may influence the chemistry of a discharge in the mixture $N_2$–$O_2$ is oxygen dissociation. The $N_2(A)$ metastable state may directly dissociate the oxygen molecule through reaction R11 (see table 2). For the present discharge conditions this process always contributes less than 2% to the total dissociation of $O_2$, the higher percentage corresponding to mixtures close to air composition, 80% $N_2$–20% $O_2$. This result is close to that

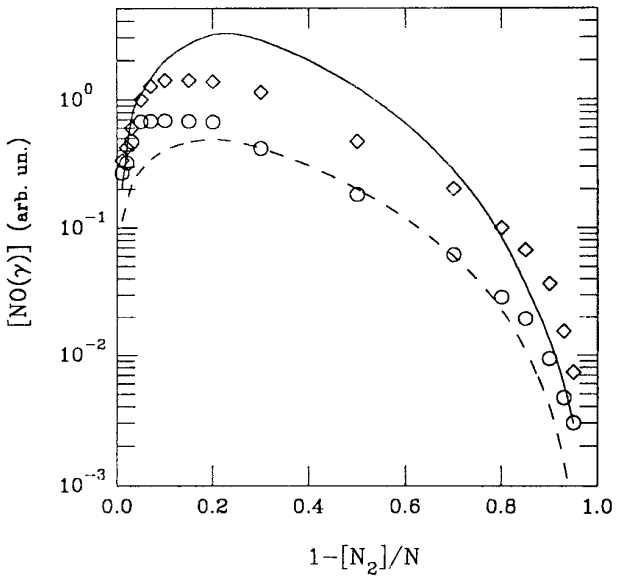


**Figure 10.** Calculated populating rate of NO($A\,^2\Sigma^+$) state and measured relative intensity of the NO($\gamma$) band at 237 nm, for the same conditions as figure 9, for $I = 30$ (– –, ○) and 80 mA (—, ◇). The symbols correspond to experimental data from [14].

reported in [44] for ozonisers. However, the $N_2(A)$ metastables may still have an indirect contribution to the production of O atoms. In fact, a major reaction for the dissociation of oxygen involves the $N_2(B)$ state,

$$N_2(B) + O_2 \rightarrow N_2(X) + O + O \qquad (22)$$

and the two nitrogen excited states $N_2(A)$ and $N_2(B)$ are strongly correlated. According to our calculations, reaction (22) may ensure up to 30% of the total dissociation rate of $O_2$ molecules, the maximum contribution being again for mixtures containing ~80% $N_2$.

Finally, it is worth mentioning that $N_2(A)$ is a possible source of $N_2O$, by the reaction

$$N_2(A) + O_2 \longrightarrow N_2O + O. \qquad (23)$$

The species $N_2O$ has importance in aeronomic research, but it was not considered in the model due to its minor influence under the discharge conditions treated here. Reaction (23) was shown to be an important source of $N_2O$ for high-pressure discharges in [45, 46], at early times during discharge development. However, in [47] it was established, for a flowing afterglow at low pressures, that the quenching of $N_2(A\,^3\Sigma_u^+, v \leqslant 2)$ by molecular oxygen is a negligible source of $N_2O$. Therefore, according to [47] $N_2(A)$ cannot be considered as a source of nitrous oxide in the upper atmosphere, unless there is a dramatic branching ratio increase with increasing vibrational excitation of $N_2(A)$ and higher vibrational levels ($v \gg 2$) are involved.

### *3.3. Gas heating*

In a stationary nitrogen discharge the main gas heating channel usually results from the exothermic reactions involving the relaxation of the vibrational levels $N_2(X\,^1\Sigma_g^+, v)$, in non-resonant V–V energy exchanges, equation (3), and V–T

processes in collisions with both $N_2$ molecules and N atoms, equations (5) and (7), respectively. However, the pooling reactions of $N_2(A)$ metastables, corresponding to equations (9) and (10), are known to play a role in the gas heating at the first instants of the discharge, before a stationary situation is reached [48, 49]. Thus, in order to verify under which conditions these reactions may become important in a stationary discharge, we have included the gas thermal balance equation (2) in the model for nitrogen, including not only processes (3), (5) and (7), but also other processes leading to gas heating such as electron elastic energy losses, electron rotational excitation followed by relaxation to the translational mode ($R$–$T$) and the reactions (9) and (10) of pooling of $N_2(A)$. According to [49–51], we have assumed that half of the energy available in the reactions goes to the translational mode, while the other is transformed into vibrational energy, which corresponds to $v_1 = 8$ and $\Delta E_1 = 2.0$ eV in equation (9), and to $v_2 = 2$ and $\Delta E_2 = 0.4$ eV in equation (10). This assumption nearly corresponds to an energy balance model in which the reactions obey the Franck–Condon principle [49]. The model further includes a module to treat the discharge under the electrodynamic point of view as presented in [52, 53], which allow us to describe axially the plasma column.

We applied the model to a surface-wave sustained discharge in nitrogen under two different conditions. The first one, I, corresponds to a discharge at $p = 0.5$ Torr, $\omega/(2\pi) = 500$ MHz in a Pyrex glass tube with inner and outer radii $a = 2.25$ cm and $b = 2.5$ cm, respectively; the second one, II, is for $p = 0.6$ Torr, $\omega/(2\pi) = 2.45$ GHz, in a quartz tube with $a = 0.75$ cm and $b = 0.9$ cm. For the first case, at 500 MHz, the electron density decreases from $4.7\times10^{10}$ cm$^{-3}$ at the launcher to $\sim3\times10^{9}$ cm$^{-3}$ at the column end, and the reduced effective electric field $E_{eff}/N$ varies in the range $7.1\times10^{-16}$–$7.6\times10^{-16}$ V cm$^2$; for the second case, at 2.45 GHz, the electron density goes from $10^{12}$ cm$^{-3}$ to $\sim4\times10^{10}$ cm$^{-3}$ and $E_{eff}/N$ is in the range $8.9\times10^{-16}$–$1.2\times10^{-15}$ V cm$^2$. Therefore, for case II we have significantly more energetic electrons, which provide a higher population of the metastable states. Consequently, the nature of gas heating changes, as shown in figures 11 and 12. Figure 11 shows the percentage contribution of the different gas heating channels to the total gas heating in the discharge, as a function of the axial position in the column, for case I. The results are normalized to the total discharge length, so that $\Delta z/L = 0$ and $\Delta z/L = 1$ correspond to the discharge end and to the launcher, respectively. Figure 12 shows the same type of data as in figure 11 but for case II. As we can see, in the case of the lower electron density and electron energy conditions of figure 11, gas heating comes essentially from the vibrational deactivation of $N_2(X, v)$ molecules in collisions with N atoms and from the non-resonant V–V exchanges, as usually stated in the literature (e.g. [54]). However, for the conditions referred to in case II, the gas heating channel associated with the reactions of pooling of $N_2(A)$ dominates. The comparison between the calculated and measured gas temperatures in II has confirmed the need for an important gas heating source coming from the pooling of metastable states [55].

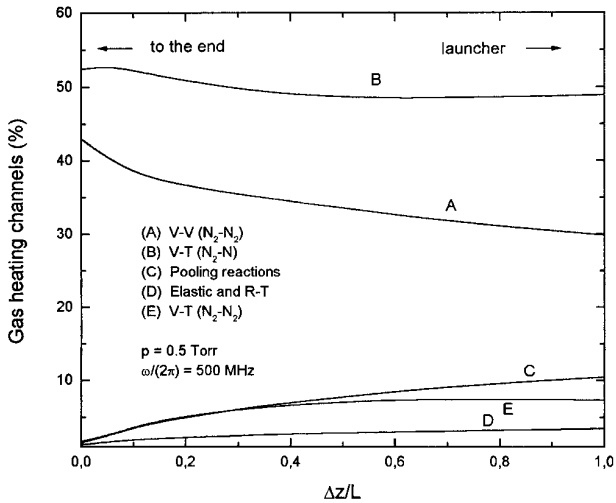


**Figure 11.** Percentage contribution of the different gas heating channels to the total gas heating, for a surface-wave discharge in pure nitrogen at $p = 0.5$ Torr, $f = 500$ MHz, inner radius $a = 2.25$ cm and external radius $b = 2.5$ cm.

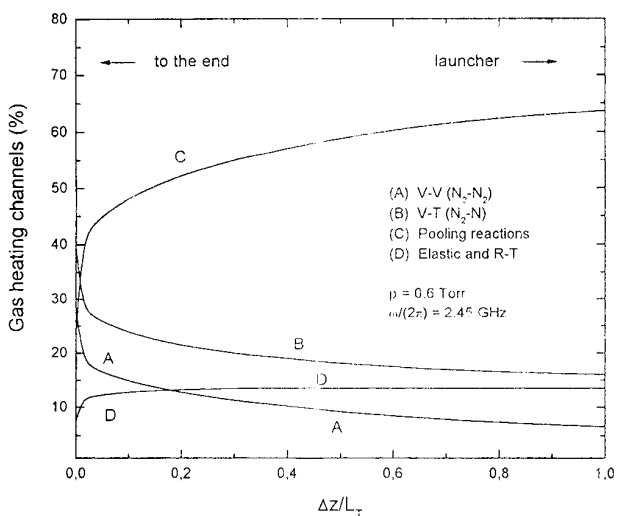


**Figure 12.** As in figure 11, but for $p = 0.6$ Torr, $f = 2.45$ GHz, inner radius $a = 0.75$ cm and external radius $b = 0.9$ cm.

## 4. Conclusions

With the aim of studying the role of the $N_2(A\,^3\Sigma_u^+)$ metastable state in a stationary low-pressure discharge in $N_2$ and $N_2$–$O_2$ mixtures, we have reported here some significant results derived from a kinetic model based on the coupled solutions to the homogeneous electron Boltzmann equation and a system of rate balance equations for the most important neutral and charged species produced in the discharge, in which the maintaining electric field is self-consistently determined. In a final section, the gas thermal balance equation is also coupled to the model. We have shown that the $N_2(A\,^3\Sigma_u^+)$ state is of capital importance in the processes of associative ionization in pure nitrogen, which are the dominant ionization mechanisms under these conditions, through the reaction $N_2(A) + N_2(a') \rightarrow e + N_4^+$ in parallel with $N_2(a') + N_2(a') \rightarrow e + N_4^+$. In the case of an $N_2$–$O_2$ mixture this state is strongly quenched by O, $O_2$ and NO, which results in an increase of the reduced

sustaining electric field of the discharge when small amounts of oxygen are added into a nitrogen discharge. We have further shown that in pure nitrogen the kinetics of $N_2(A)$ is strongly coupled to that of $N_2(B)$ and N atoms, through the reactions $N_2(B) + N_2 \rightarrow N_2(A) + N_2$, $N_2(A) + N_2(X, 5 \leqslant v \leqslant 14) \rightarrow N_2(B) + N_2(X, v = 0)$ and $N_2(A) + N \rightarrow N_2(X, 6 \leqslant v \leqslant 9) + N$. On the other hand, in the case of a discharge in $N_2$–$O_2$ the metastable $N_2(A\,^3\Sigma_u^+)$ is involved in one of the main reactions for NO formation, $N_2(A) + O \rightarrow NO + N(^2D)$, and it is responsible for the emission of NO $\gamma$ bands from NO(A), through collisions $N_2(A) + NO(X) \rightarrow N_2(X) + NO(A)$. Finally, we have also shown that $N_2(A)$ may give a significant contribution to the gas heating in a nitrogen discharge, for conditions of simultaneously high electron density and electron mean energy, such as those present in a microwave discharge at high field frequency and small tube radius. In summary, we want to stress that even if the vibrational states $N_2(X\,^1\Sigma_g^+, v)$ are the main energy reservoirs in a nitrogen discharge, the metastable state $N_2(A\,^3\Sigma_u^+)$ plays a crucial role in the physics of $N_2$ and $N_2$–$O_2$ discharges, in such fundamental aspects as ionization, chemistry and gas heating.

## References


[1] Capitelli M (ed) 1996 *Molecular Physics and Hypersonic Flows (NATO ASI Series)* vol C-482 (Dordrecht: Kluwer)

[2] Katu I, Noguchi K and Numada K 1989 Preparation of silicon nitride films at room temperature using double-tubed coaxial line-type microwave plasma chemical vapor deposition system *J. Appl. Phys.* **62** 492–7

[3] Benedictis S D, Dilecce G and Simek M 1997 The NO($A\,^2\Sigma^+$) excitation mechanism in a $N_2$–$O_2$ pulsed RF discharge *J. Phys. D: Appl. Phys.* **30** 2887–94

[4] Granier A, Chéreau D, Henda K, Safari R and Leprince P 1994 Validity of actinometry to monitor oxygen atom concentration in microwave discharges created by surface wave in $O_2$–$N_2$ discharges *J. Appl. Phys.* **75** 104–14

[5] Cacciatore M, Capitelli M and Gorse C 1982 Non-equilibrium dissociation and ionization of nitrogen in electrical discharges: the role of electronic collisions from vibrationally excited molecules *Chem. Phys.* **66** 141–51

[6] Loureiro J and Ferreira C M 1986 Coupled electron energy and vibrational distribution functions in stationary $N_2$ discharges *J. Phys. D: Appl. Phys.* **19** 17–35

[7] Gorse C, Cacciatore M, Capitelli M, de Benedictis S and Dilecce G 1988 Electron energy distribution functions under $N_2$ discharge and post-discharge conditions: a self-consistent approach *Chem. Phys.* **119** 63–70

[8] Nagpal R and Ghosh P K 1990 Electron energy distribution functions and vibrational population densities of excited electronic states in DC discharges through nitrogen *J. Phys. D: Appl. Phys.* **23** 1663–70

[9] Loureiro J 1991 Dissociation rate and N($^4$S) atom concentrations in a $N_2$ glow-discharge *Chem. Phys.* **157** 157–68

[10] Guerra V and Loureiro J 1997 Electron and heavy particle kinetics in a low pressure nitrogen glow discharge *Plasma Sources Sci. Technol.* **6** 361–72

[11] Gordiets B and Ricard A 1993 Production of N, O and NO in $N_2$–$O_2$ flowing discharges *Plasma Sources Sci. Technol.* **2** 158–63

[12] Nahorny J, Ferreira C M, Gordiets B, Pagnon D, Touzeau M and Vialle M 1995 Experimental and theoretical investigation of a $N_2$–$O_2$ dc flowing glow discharge *J. Phys. D: Appl. Phys.* **28** 738–47

[13] Guerra V and Loureiro J 1995 Non-equilibrium coupled kinetics in stationary $N_2$–$O_2$ discharges *J. Phys. D: Appl. Phys.* **28** 1903–18

[14] Gordiets B F, Ferreira C M, Guerra V L, Loureiro J M A H, Nahorny J, Pagnon D, Touzeau M and Vialle M 1995 Kinetic model of a low-pressure $N_2$–$O_2$ flowing glow discharge *IEEE Trans. Plasma. Sci.* **23** 750–67

[15] Guerra V and Loureiro J 1997 Self-consistent electron and heavy-particle kinetics in a low pressure $N_2$–$O_2$ glow discharge *Plasma Sources Sci. Technol.* **6** 373–85

[16] Guerra V and Loureiro J 1999 Kinetic model of a low pressure microwave discharge in $O_2$–$N_2$ including the effects of $O^-$ ions on the characteristics for plasma maintenance *Plasma Sources Sci. Technol.* **6** 373–85

[17] Benedictis S D, Dilecce G and Simek M 1993 Time-resolved LIF spectroscopy on $N_2(A)$ metastable in a He/$N_2$ pulsed rf discharge *Chem. Phys.* **178** 547–60

[18] Marković V L, Pejović M M and Petrović Z L 1994 Kinetics of activated nitrogen states in late afterglow by the time-delay method **27** 979–84

[19] Augustyniak E and Borysow J 1994 Kinetics of the ($A\,^3\Sigma_u^+$, $v = 0$) state of $N_2$ in the near afterglow of a nitrogen pulsed discharge *J. Phys. D: Appl. Phys.* **27** 652–60

[20] Piper L G 1989 The excitation of $N_2(B\,^3\Pi_g, v' = 1$–$12)$ in the reaction between $N_2(A\,^3\Sigma_u^+)$ and $N_2(X, v \geqslant 5)$ *J. Chem. Phys.* **91** 864–73

[21] Dilecce G and Benedictis D S 1999 Experimental studies on elementary kinetics in $N_2$–$O_2$ pulsed discharges *Plasma Sources Sci. Technol.* **8** 266–78

[22] Benedictis S D and Dilecce G 1995 Vibrational relaxation of $N_2(C, v)$ state in $N_2$ pulsed rf discharge: electron impact and pooling reactions *Chem. Phys.* **19** 149–62

[23] Supiot P, Blois D, Benedictis S D, Dilecce G, Barj M, Chapput A, Dessaux O and Goudmand P 1999 Excitation of $N_2(B\,^3\Pi_g)$ in the nitrogen short-lived afterglow *J. Phys. D: Appl. Phys.* **32** 1887–93

[24] Foissac C, Campargue A, Kachanov A, Supiot P, Weirauch G and Sadeghi N 2000 Intracavity laser absorption spectroscopy applied to measure the absolute density and temperature of $N_2(A\,^3\Sigma_u^+)$ metastable molecules in a flowing $N_2$ microwave discharge *J. Phys. D: Appl. Phys.* **33** 2434–41

[25] Ferreira C M and Loureiro J 1989 Electron excitation rates and transport parameters in high-frequency $N_2$ discharges *J. Phys. D: Appl. Phys.* **22** 76–82

[26] Sá P A, Loureiro J and Ferreira C M 1992 Effects of electron–electron collisions on the characteristics of dc and microwave discharges in argon at low pressures *J. Phys. D: Appl. Phys.* **25** 960–6

[27] Gousset G, Ferreira C M, Pinheiro M, Sá P A, Touzeau M, Vialle M and Loureiro J 1991 Electron and heavy-particle kinetics in the low pressure oxygen positive column *J. Phys. D: Appl. Phys.* **24** 290–300

[28] Ferreira C M, Gousset G and Touzeau M 1988 Quasi-neutral theory of positive columns in electronegative gases *J. Phys. D: Appl. Phys.* **21** 1403–13

[29] Hirshfelder J O, Curtiss C F and Bird R B 1964 *Molecular Theory of Gases and Liquids* (New York: Wiley)

[30] Lofthus A and Krupenie P H 1977 The spectrum of molecular nitrogen *J. Phys. Chem. Ref. Data* **6** 113

[31] Cernogora G, Houchard L, Touzeau M and Ferreira C M 1981 Population of $N_2(A\,^3\Sigma_u^+)$ metastable states in a pure nitrogen glow discharge *J. Phys. B: At. Mol. Phys.* **14** 2977–87

[32] Cernogora G, Ferreira C M, Houchard L, Touzeau M and Loureiro J 1984 Vibrational populations of $N_2(A\,^3\Sigma_u^+)$ in a pure nitrogen glow discharge *J. Phys. B: At. Mol. Phys.* **17** 4429–37

[33] Ferreira C M, Houchard M T L and Cernogora G 1984 Vibrational populations of $N_2(B\,^3\Pi_g)$ in a pure nitrogen glow discharge *J. Phys. B: At. Mol. Phys.* **17** 4439–48

[34] Polak L S, Sergeev P A and Slovetskii D I 1977 Nitrogen ionization mechanism in a glow discharge *High Temp.* **15** 13–20

[35] Golubovskii Y B and Telezhko V M 1984 Ionization processes in a nitrogen discharge at medium pressures *High Temp.* **22** 340–8

[36] Bol'shakova L G, Golubovskii Y B, Telezhko V M and Stoyanov D G 1990 Mechanism for ionization of nitrogen molecules in self-sustained discharges *Sov. Phys.–Tech. Phys.* **35** 665–8

[37] Brunet H, Vincent P and Rocca-Serra J 1983 Ionization mechanism in a nitrogen glow discharge *J. Appl. Phys.* **54** 4951–7

[38] Brunet H and Rocca-Serra J 1985 Model for a glow discharge in flowing nitrogen *J. Appl. Phys.* **57** 1574–81

[39] Berdyshev A V, Kochetov I V and Napartovich A P 1988 Ionization mechanism in a quasisteady glow discharge in pure nitrogen *Sov. J. Plasma Phys.* **14** 438–40

[40] Paniccia F, Gorse C, Cacciatore M and Capitelli M 1987 Nonequilibrium ionization of nitrogen: the role of stepwise ionization from metastable states in the presence of superelastic electronic collisions *J. Appl. Phys.* **61** 3123–6

[41] Wedding A B, Borysow J and Phelps A V 1993 $N_2(a''^1\Sigma_g^+)$ metastable collisional destruction and rotational excitation transfer by $N_2$ *J. Chem. Phys.* **98** 6227–34

[42] Loureiro J, Sá P A and Guerra V 2001 Role of long-lived $N_2(X'^1\Sigma_g^+, v)$ molecules and $N_2(A^3\Sigma_u^+)$ and $N_2(A^3\Sigma_u^+)$ states in the light emissions of a $N_2$ afterglow *J. Phys. D: Appl. Phys.* at press

[43] Heidner R F, Sutton D G and Suchard S N 1976 Kinetic study of $N_2(B^3\Pi_g, v)$ quenching by laser-induced fluorescence *Chem. Phys. Lett.* **37** 243–8

[44] Eliasson B, Kogelschatz U and Baessler P 1984 Dissociation of $O_2$ in $N_2/O_2$ mixtures *J. Phys. B: At. Mol. Phys.* **17** L797–L801

[45] Eliasson B and Kogelschatz U 1986 *J. Chim. Physique.* **83** 279–82

[46] Kogelschatz U, Eliasson B and Egli W 1997 Dielectric-barrier discharges. Principles and applications *J. Physique. IV* **7** C4–47

[47] Fraser M E and Piper L G 1989 Product branching ratios from the $N_2(A^3\Sigma_u^+) + O_2$ interaction *J. Phys. Chem.* **93** 1107–11

[48] Bogatov N A, Borodachova T V, Gitlin M S, Golubev S V, Polushkin I N and Razin S V 1986 The study of population dynamics of vibrational levels of $N_2(A^3\Sigma_u^+)$ states in a gas discharge by intracavity laser spectroscopy (ICLS) technique *Proc. 8th European Sectional Conf. Atomic and Molecular Physics of Ionized Gases (Greifswald, German Democratic Republic)* pp 386–7

[49] Boeuf J P and Kunhardt E E 1986 Energy balance in a nonequilibrium weakly ionized nitrogen discharge *J. Appl. Phys.* **60** 915–23

[50] Gorse C and Capitelli M 1987 Coupled electron and excited-state kinetics in a nitrogen afterglow *J. Appl. Phys.* **62** 4072–6

[51] Dhali S K and Low L H 1988 Transient analysis of bulk nitrogen glow discharge *J. Appl. Phys.* **64** 2917–26

[52] Dias F M, Tatarova E, Henriques J and Ferreira C M 1999 Experimental investigation of surface wave propagation in collisional plasma columns *J. Appl. Phys.* **85** 2528–33

[53] Tatarova E, Dias F M, Ferreira C M and Ricard A 1999 On the axial structure of a nitrogen surface wave sustained discharge: theory and experiment *J. Appl. Phys.* **85** 49–62

[54] Gordiets B F, Ferreira C M, Pinheiro M J and Ricard A 1998 Self-consistent kinetic model of low-pressure $N_2$–$H_2$ flowing discharges: I. Volume processes *Plasma Sources Sci. Technol.* **7** 363–78

[55] Guerra V, Tatarova E, Dias F M and Ferreira C M 2000 Influence of metastable excited states in the gas heating of a surface-wave sustained nitrogen discharge *Europhysics Conf. Abstracts: XVth Europhysics Conf. Atomic and Molecular Physics of Ionized Gases (Miskolc-Lillafured, Hungary)* (European Physical Society) pp 218–19